

# PPAR $\alpha$ Deficiency in Inflammatory Cells Suppresses Tumor Growth

Arja Kaipainen<sup>1</sup>, Mark W. Kieran<sup>1,2</sup>, Sui Huang<sup>1</sup>, Catherine Butterfield<sup>1</sup>, Diane Bielenberg<sup>1</sup>, Gustavo Mostoslavsky<sup>3</sup>, Richard Mulligan<sup>3</sup>, Judah Folkman<sup>1</sup>, Dipak Panigrahy<sup>1\*</sup>

<sup>1</sup> Vascular Biology Program, Department of Surgery, Children's Hospital, Harvard Medical School, Boston, Massachusetts, United States of America,

<sup>2</sup> Department of Pediatric Oncology, Dana-Farber Cancer Institute, Harvard Medical School, Boston, Massachusetts, United States of America,

<sup>3</sup> Department of Genetics, Harvard Medical School, Boston, Massachusetts, United States of America

**Inflammation in the tumor bed can either promote or inhibit tumor growth. Peroxisome proliferator-activated receptor (PPAR) $\alpha$  is a central transcriptional suppressor of inflammation, and may therefore modulate tumor growth. Here we show that PPAR $\alpha$  deficiency in the host leads to overt inflammation that suppresses angiogenesis via excess production of the endogenous angiogenesis inhibitor thrombospondin-1 and prevents tumor growth. Bone marrow transplantation and granulocyte depletion show that PPAR $\alpha$  expressing granulocytes are necessary for tumor growth. Neutralization of thrombospondin-1 restores tumor growth in PPAR $\alpha$ -deficient mice. These findings suggest that the absence of PPAR $\alpha$  activity renders inflammatory infiltrates tumor suppressive and, thus, may provide a target for inhibiting tumor growth by modulating stromal processes, such as angiogenesis.**

Citation: Kaipainen A, Kieran MW, Huang S, Butterfield C, Bielenberg D, et al (2007) PPAR $\alpha$  Deficiency in Inflammatory Cells Suppresses Tumor Growth. PLoS ONE 2(2): e260. doi:10.1371/journal.pone.0000260

## INTRODUCTION

Non-neoplastic "host" cells, such as endothelial, stromal and inflammatory cells, play a critical role in tumor growth; and genes prognostic for cancer outcome may be expressed in the non-neoplastic tissue compartment [1]. While tumor angiogenesis has been intensely studied for more than two decades and has become an accepted target in cancer therapy, it is only in the last few years that inflammation has entered center stage of investigations into non-cell autonomous processes in cancer.

Chronic inflammation in the tumor stroma has long been known to contribute to tumor progression. Increased infiltration of innate immune cells to the tumor, such as macrophages, mast cells and neutrophils, correlates with increased angiogenesis and poor prognosis [2,3]. In contrast, lymphocytic/monocytic inflammatory infiltrates are sometimes associated with tumor inhibition and a more favorable prognosis [3–5]. Recently, NF- $\kappa$ B, a central positive regulator of inflammation, has emerged as a molecular link between inflammation and cancer growth. NF- $\kappa$ B promotes tumor growth not only in a cancer cell-autonomous manner by transactivating anti-apoptotic genes, but it also stimulates inflammatory processes in the microenvironment that lead to the production of tumor-promoting cytokines [6].

Conversely, PPAR $\alpha$ , a ligand-activated nuclear receptor/transcription factor, is a key negative regulator of inflammation. Activation of PPAR $\alpha$  by ligands inhibits inflammation [7] whereas PPAR $\alpha$  deficient mice exhibit enhanced inflammation [8]. Despite PPAR $\alpha$ 's role in suppressing inflammation, it appears to be necessary and sufficient for rodent tumorigenesis [9]. In fact, prolonged PPAR $\alpha$  activation by peroxisome proliferators induces hepatocarcinogenesis in rodents; conversely PPAR $\alpha$  KO mice are resistant to tumorigenesis induced by PPAR $\alpha$  agonists [10,11]. This may be due in part to cell-autonomous effect of PPAR $\alpha$ , because it is expressed in many tumor cell lines [12,13]. Another possibility is that in PPAR $\alpha$  deficient mice, stromal processes, such as inflammation, inhibit tumor growth, which results in microscopic-sized tumors that remain dormant. The role of PPAR $\alpha$  in inflammation has been extensively studied in normal physiological processes (wound healing) and cardiovascular diseases (atherosclerosis) [14,15]; but the effect of PPAR $\alpha$  mediated suppression of

inflammation on tumors has not been characterized. Here we show that overt inflammation in the absence of PPAR $\alpha$  in the host tissue prevents tumor growth. This indicates that in contrast to the emerging notion that inflammatory infiltrates promote tumors, the specific nature of the inflammatory process must be considered when linking inflammation to tumorigenesis.

## RESULTS

### Deletion of PPAR $\alpha$ in Host Tissue inhibits Tumor Growth and Metastasis

We used several murine models to determine how the increased inflammatory response observed in the absence of PPAR $\alpha$  affects tumor growth and metastasis. First, we stably transformed mouse embryonic fibroblasts (MEF) with SV40 large T antigen and H-ras [16] to obtain isogenic tumorigenic cell lines that were either wild type (PPAR $\alpha$ (+/+)MEF/RS) or lacked PPAR $\alpha$  (PPAR $\alpha$ (–/–)MEF/RS). These two tumorigenic cell lines allowed us to distinguish between the tumor cell- autonomous role and the host tissue role of PPAR $\alpha$ . We found that the growth of these isogenic tumors derived from both cell lines was almost completely suppressed in KO host mice that lacked PPAR $\alpha$ , but not in WT

**Academic Editor:** Mikhail Blagosklonny, Ordway Research Institute, Inc., United States of America

**Received** October 16, 2006; **Accepted** February 2, 2007; **Published** February 28, 2007

**Copyright:** © 2007 Kaipainen et al. This is an open-access article distributed under the terms of the Creative Commons Attribution License, which permits unrestricted use, distribution, and reproduction in any medium, provided the original author and source are credited.

**Funding:** This study was supported by the Stop & Shop Pediatric Brain Tumor Fund and the C.J. Buckley Pediatric Brain Tumor Research Fund (M.K.) and Department of Defense Innovator Award #W81XWH-04-1-0316 and private philanthropic funds (J.F.).

**Competing Interests:** The authors have declared that no competing interests exist.

**\* To whom correspondence should be addressed.** E-mail: dipak.panigrahy@childrens.harvard.edu

animals,  $p < 0.0001$  (Figures 1A and 1B). Although tumors derived from MEFs deficient of PPAR $\alpha$  were partially suppressed in WT animals (by 41%), indicating a cell-autonomous role of PPAR in tumor growth, a drastic effect in tumor suppression was observed when the host was PPAR $\alpha$  deficient both in the case of PPAR $\alpha$ (+/+) tumors (87% suppression) as well as PPAR $\alpha$ (-/-) tumors (97% suppression) (Figure 1C). These results suggest that the presence of PPAR $\alpha$  gene in the host animals is essential for tumor growth.

To examine the role of established tumor murine models we first used WT and KO mice derived from WT (S1)  $\times$  KO (S4) crossmating. The growth of B16-BL6 tumor was almost completely inhibited in the PPAR $\alpha$  KO (S1/S4) host, but was not affected in PPAR $\alpha$  WT (S1/S4) animals,  $p < 0.0001$  (Figure 1D). This result suggests that presence of the PPAR $\alpha$  gene in the host tissue is essential to support tumor growth.

Given that the above results clearly suggest that the status of the PPAR $\alpha$  locus in the host affects tumor growth, we next evaluated the growth of three PPAR $\alpha$ -positive murine tumor models in PPAR $\alpha$  KO (S4) animals, including Lewis lung carcinoma (LLC), metastatic B16-F10/GFP melanoma, and B16-BL6 melanoma,  $p < 0.001$  (Figure 1E–G). LLC tumors have been reported to grow aggressively at similar rates in the Sv129, C57BL/6 and Sv129/C57BL/6 strains without evidence of transplantation immunity. This suggests that disparity in either minor or major immunohistocompatibility genes does not affect tumor growth in these models [17] (Figure S1). Macroscopic growth of LLC and B16-F10/GFP tumors was completely suppressed in PPAR $\alpha$  KO mice, even when mice were monitored for more than 100 days post implantation (Figure 1E–G). Similarly, tumor metastasis was also suppressed in PPAR $\alpha$  KO mice. When B16-F10/GFP melanoma

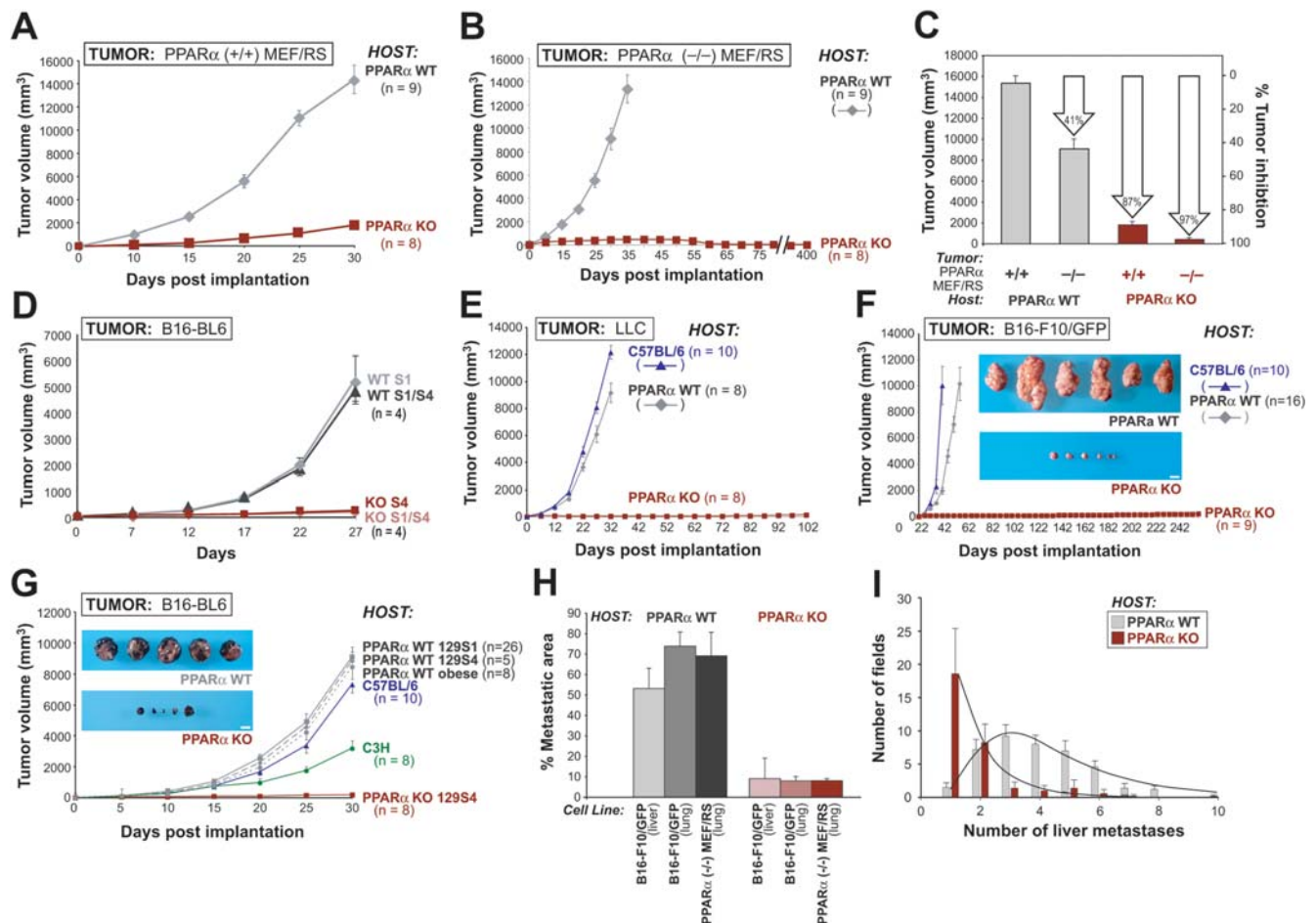


**Figure 1.** Tumor growth and metastasis are inhibited in PPAR $\alpha$  knockout (KO) mice. PPAR $\alpha$  wild type (WT) and PPAR $\alpha$  KO mice were injected subcutaneously or intravenously with various tumor cell lines; (n) = number of mice/group. (A–C) The growth of engineered PPAR $\alpha$ (+/+) MEF/RS and PPAR $\alpha$ (-/-) MEF/RS tumors in PPAR $\alpha$  WT and KO mice. (A) PPAR $\alpha$ (+/+) MEF/RS tumor growth in PPAR $\alpha$  WT (◆ gray) and KO (■ brown) mice. (B) The growth curves of PPAR $\alpha$ (-/-) MEF/RS in PPAR $\alpha$  WT (◆ gray) and KO (■ brown) mice. (C) Columns summarize the inhibitory effect of PPAR $\alpha$  (-/-) tumor and host cells at day 30 post implantation (average  $\pm$  standard error of the mean). (D–F) The growth of different murine tumors in different mouse strains. (D) The growth of B16-BL6 melanoma was compared in WTS1 (◆ gray), WTS1/S4 (▲ gray), KOS4 (■ brown) and KO S1/S4 (◆ pink) strains. WT S1/S4, PPAR $\alpha$  WT second generation littermates from PPAR $\alpha$  WT 129/S1 and KO 129/S4; KO S1/S4, PPAR $\alpha$  KO second generation littermates from PPAR $\alpha$  KO 129/S4. (E) Lewis lung carcinoma growth in PPAR $\alpha$  WT (◆ gray), PPAR $\alpha$  KO (■ brown) and C57BL/6 (▲ blue) mice. (F) B16-F10/GFP tumor growth in PPAR $\alpha$  WT, PPAR $\alpha$  KO and C57BL/6 mice, blue insets demonstrate representative B16-F10/GFP tumors in PPAR $\alpha$  WT and KO mice on day 30 post implantation. Scale bar, 1 cm. (G) B16-BL6 melanoma was implanted in mice of indicated genetic backgrounds. Representative B16-BL6 tumors in PPAR $\alpha$  WT (◆ gray) and PPAR $\alpha$  KO (■ brown) mice on day 30 post implantation are shown (blue insets). Scale bar, 1 cm. (H–I) Metastasis in PPAR $\alpha$  WT and KO mice. H: Metastatic areas of B16-F10/GFP and PPAR $\alpha$ (-/-) MEF/RS tumor cells at day 21 post-injection in lung and liver of PPAR $\alpha$  WT (◆ gray) and KO mice (■ brown). I: Number of liver metastases in PPAR $\alpha$  WT (◆ gray) and KO (■ brown) mice injected with B16-F10/GFP tumor cells (average  $\pm$  standard deviation).

doi:10.1371/journal.pone.0000260.g001



cells and engineered PPAR $\alpha$  deficient tumor cells, PPAR $\alpha$  ( $-/-$ ) MEF/RS (see below) were injected via tail vein, 21 out of 21 PPAR $\alpha$  wild-type (WT) mice died of lung and/or liver metastasis by day 21. In contrast, the PPAR $\alpha$  KO hosts suppressed metastatic growth in lung and liver, reducing the infiltration of the tumor cells from 50–70% of normal organ tissue area in the WT hosts to less than 10% tissue area in PPAR $\alpha$  KO animals (Figure 1H). Furthermore, the incidence of metastasis, as measured by the number of histologically identified metastatic foci, was strongly suppressed in PPAR $\alpha$  KO mice. The majority of microscopic fields of liver sections in PPAR $\alpha$  KO mice revealed only one or two metastases compared to 4–5 foci in livers of WT hosts (Figure 1I). Together these findings support the importance of PPAR $\alpha$  expression in host cells for tumor development.

The non-growing PPAR $\alpha$  ( $-/-$ ) MEF/RS tumors in PPAR $\alpha$  KO mice prompted us to investigate whether these tumors were just a mass of connective tissue or viable dormant microtumors, a state in which tumor cell proliferation is balanced by cell death [18,19]. Analysis of the small (<2 mm), non-growing lesions at the

injection site identified viable PPAR $\alpha$  ( $-/-$ ) MEF/RS large T antigen expressing and proliferating tumor cells (Figure 2A). When re-transplanted to PPAR $\alpha$  WT mice, these tumors grew rapidly to over 10,000 mm<sup>3</sup> (Figure 2A) indicating that PPAR $\alpha$  in the host can rescue PPAR $\alpha$   $-/-$  tumor cells. Although these findings suggest that the presence of PPAR $\alpha$  both in the tumor cells as well as in the host is necessary for unabated tumor growth, they also demonstrate that PPAR $\alpha$  in tumor cells is not necessary for tumor cell viability. Conversely, the results underscore the importance of PPAR $\alpha$  in the host tissue to sustain tumor growth.

Histological examination revealed a pronounced leukocyte infiltration (based on CD45-positive staining) in the non-necrotic stroma of all tumors grown in PPAR $\alpha$  KO mice (Figure 2B). In contrast, PPAR $\alpha$  WT animals exhibited the usual leukocytic infiltrate that was limited to necrotic areas (Figure 2B). Moreover, PECAM-1 staining performed to visualize blood capillaries revealed a decreased microvessel density in tumors from PPAR $\alpha$  KO hosts when compared to tumors from WT hosts of the same size at day 7 (data not shown), as well as at day 30 post

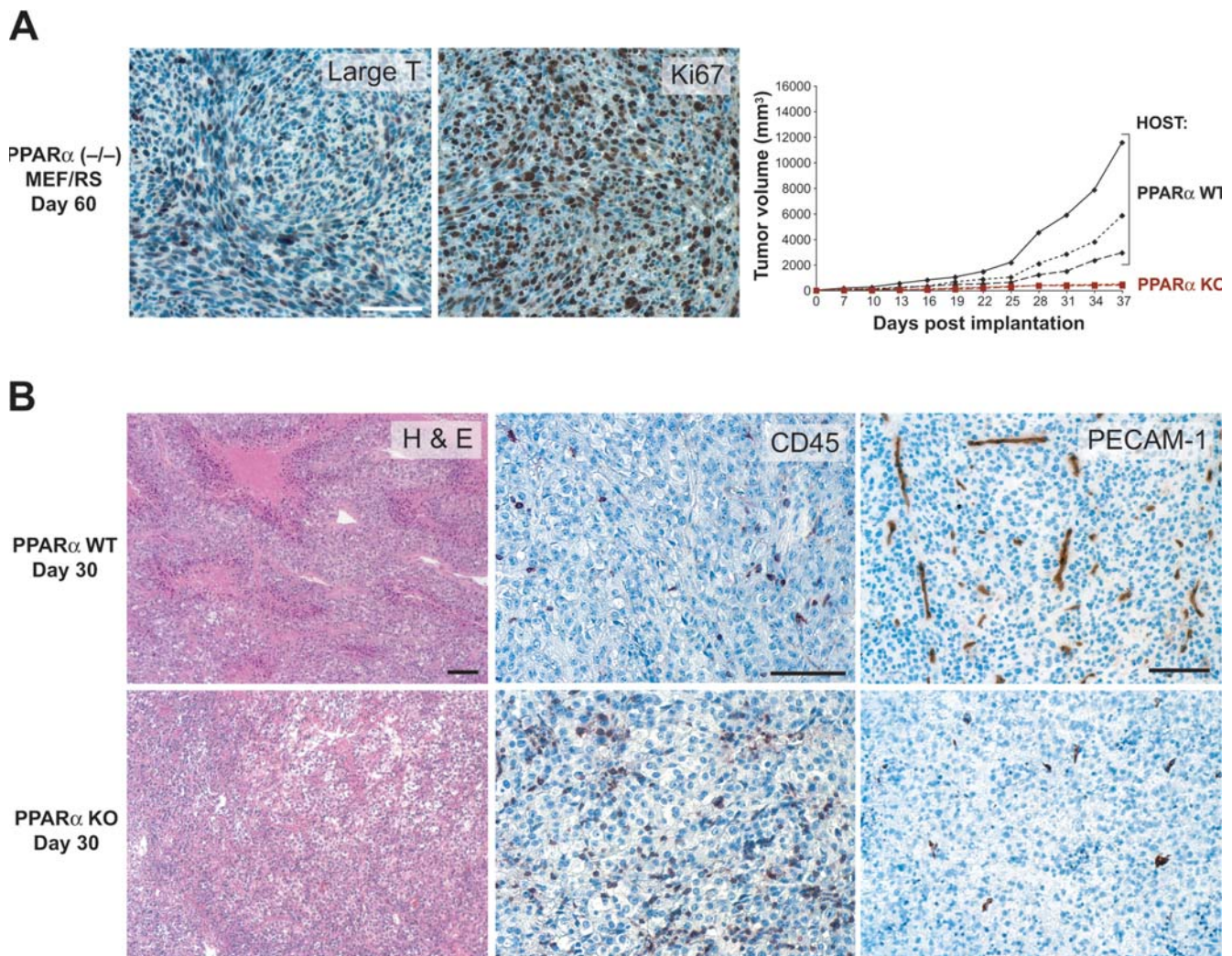


**Figure 2.** Immunohistological analysis of dormant tumors in PPAR $\alpha$  KO mice. The dormant tumors contain viable and proliferating cells, and show decreased microvessel (PECAM1) and increased leukocyte (CD45) staining. (A) Dormant PPAR $\alpha$  ( $-/-$ ) MEF/RS tumors in PPAR $\alpha$  KO mice from day 60 post-tumor implantation revealed abundant SV40 large T-antigen staining and proliferation (Ki-67). Dormant PPAR $\alpha$  ( $-/-$ ) MEF/RS tumors on day 60 were implanted as pieces (1 mm<sup>3</sup>) into PPAR $\alpha$  WT and KO mice (3 mice in each group). (B) Immunohistochemical analysis of subcutaneous B16-F10/GFP tumors (H&E, CD45/brown color, PECAM-1/brown color) from day 30 post-implantation in PPAR $\alpha$  WT mice and KO mice. Scale bars, 100  $\mu$ m. doi:10.1371/journal.pone.0000260.g002

implantation (Figure 2B). Therefore, the absence of PPAR $\alpha$  in the stromal tissue of the host appears to have two major consequences: an increase in inflammation and a decrease in tumor angiogenesis.

### Loss of Host PPAR $\alpha$ Inhibits Corneal Neovascularization and Permeability

Decreased microvessel density may reflect direct or indirect antiangiogenic effects caused by the lack of PPAR $\alpha$  activity. Because all tumors used here are known to produce the angiogenic cytokine VEGF, we first investigated whether PPAR $\alpha$  plays a role in VEGF signaling in the host cells. We employed two different *in vivo* VEGF-activity assays: VEGF-mediated, FGF2-induced corneal neovascularization, and VEGF-induced vascular permeability. Implantation of pellets containing 20 ng of FGF2 into the corneas of mice promotes the extravasation of leukocytes and stimulates VEGF-dependent corneal neovascularization [20,21]. PPAR $\alpha$  KO mice exhibited >50% inhibition of vessel length when compared to WT animals, while the initial sprouting (reflected in clock hours of the neovascularized area) was not affected (Figure 3A). Complete abrogation of angiogenesis in the WT mice in the presence of soluble VEGF-receptor-1 (VEGFR1) confirmed that angiogenesis in these WT animals was mediated by VEGF (Figure 3A), consistent with previous studies [20]. In our second approach, we evaluated whether host PPAR $\alpha$  affected VEGF-induced vascular permeability, a standard test of *in vivo* VEGF activity [22,23]. In response to VEGF, WT mice displayed

Evans blue extravasation into the subcutaneous skin and ears (Figure 3B) that was 300–400% greater than that of PPAR $\alpha$  KO mice (Figure 3B). Together, these results indicate that host PPAR $\alpha$  is indispensable for VEGF-dependent signaling.

### PPAR $\alpha$ Deficiency in Bone Marrow Cells Inhibits Tumor Growth

Given the observation that the tumor bed of PPAR $\alpha$  KO mice exhibited an increased inflammatory response, we performed reciprocal bone marrow transplantations between WT and KO mice to determine whether the hematopoietic compartment of PPAR $\alpha$  deficient mice plays a role in the inhibition of tumor growth. Bone marrow cells from WT mice were capable of restoring the “wild-type” tumor growth pattern of B16-BL6 tumors in PPAR $\alpha$  deficient hosts (Figure 4A). Conversely, PPAR $\alpha$ -deficient bone marrow cells, when transplanted into WT hosts, conferred the tumor-suppressing phenotype of PPAR $\alpha$  KO mice,  $p < 0.0001$  (Figure 4A). It is important to note that in the bone marrow transplantation protocol used, >90% of the hematopoietic system of the recipient was derived from the donor marrow (Figure S2A); this argues against the possibility that PPAR $\alpha$  KO bone marrow cells have a direct, “dominant-negative” effect that overrides a tumor promoting effect of WT bone marrow cells. Instead, the result strongly suggests that the influence of host PPAR $\alpha$  on tumor growth is conveyed solely by PPAR $\alpha$  activity in bone marrow derived cells, because in these reciprocal trans-

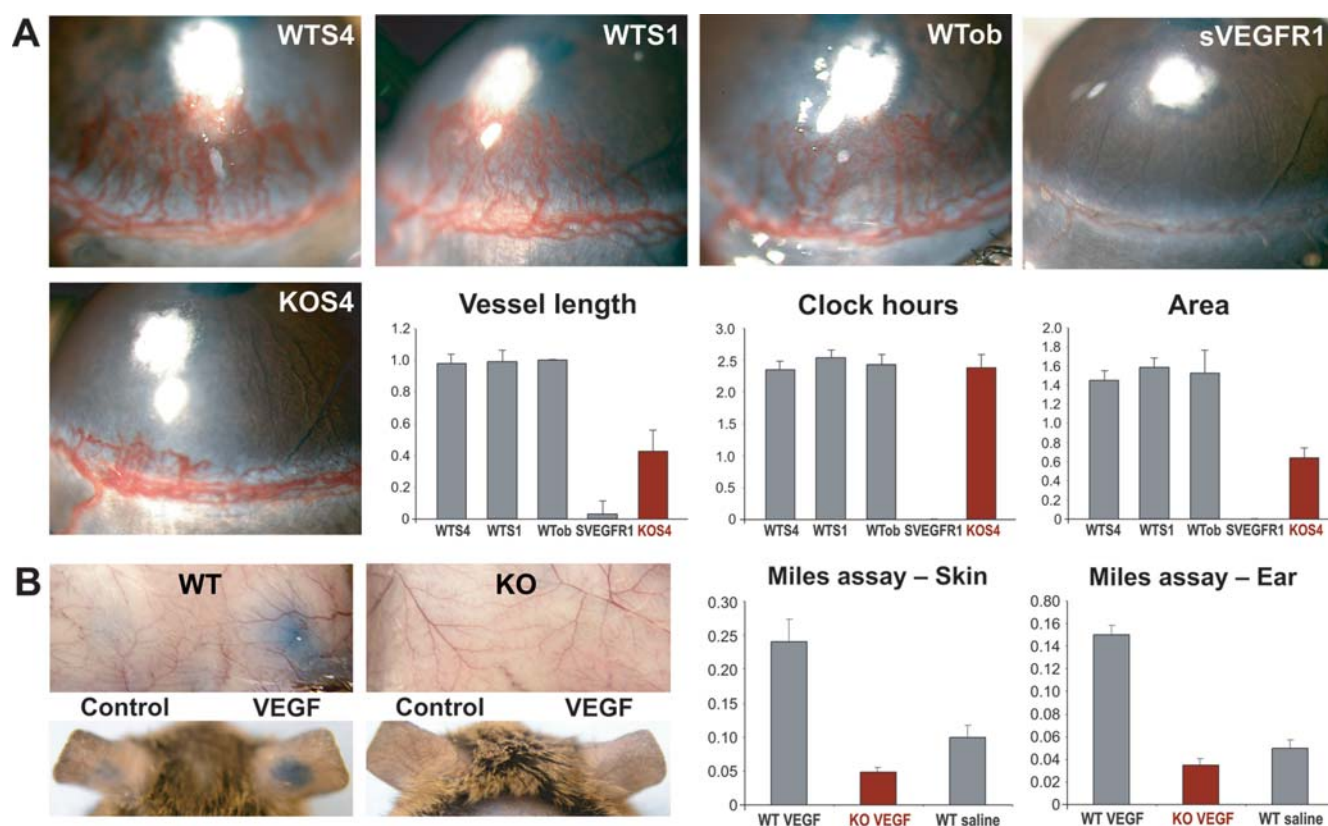


**Figure 3.** FGF2-induced corneal neovascularization and VEGF-induced vascular permeability are inhibited in PPAR $\alpha$  KO mice. (A) FGF-2 (20 ng) stimulates corneal neovascularization in WT 129S4/SvJae strain, WT 129S1/SvIMJ strain and obese WT (129S1/SvJae) mice. Soluble murine VEGFR1 completely inhibits FGF2-induced angiogenesis in WT mouse (sVEGFR1). FGF2-induced corneal neovascularization is potently suppressed in PPAR $\alpha$  KO mouse (KOS4). Vessel length, clock hours, and area of neovascularization in PPAR $\alpha$  WT and KO mice are represented in bar graphs (average  $\pm$  standard deviation). (B) Evans blue dye leakage in dorsal skin and ears after injection with VEGF or saline in PPAR $\alpha$  WT and KO mice ( $n=6$  mice/group). Spectrophotometric analysis of extravasated Evans blue of skin and ear is represented in bar graph (average  $\pm$  standard deviation). doi:10.1371/journal.pone.0000260.g003



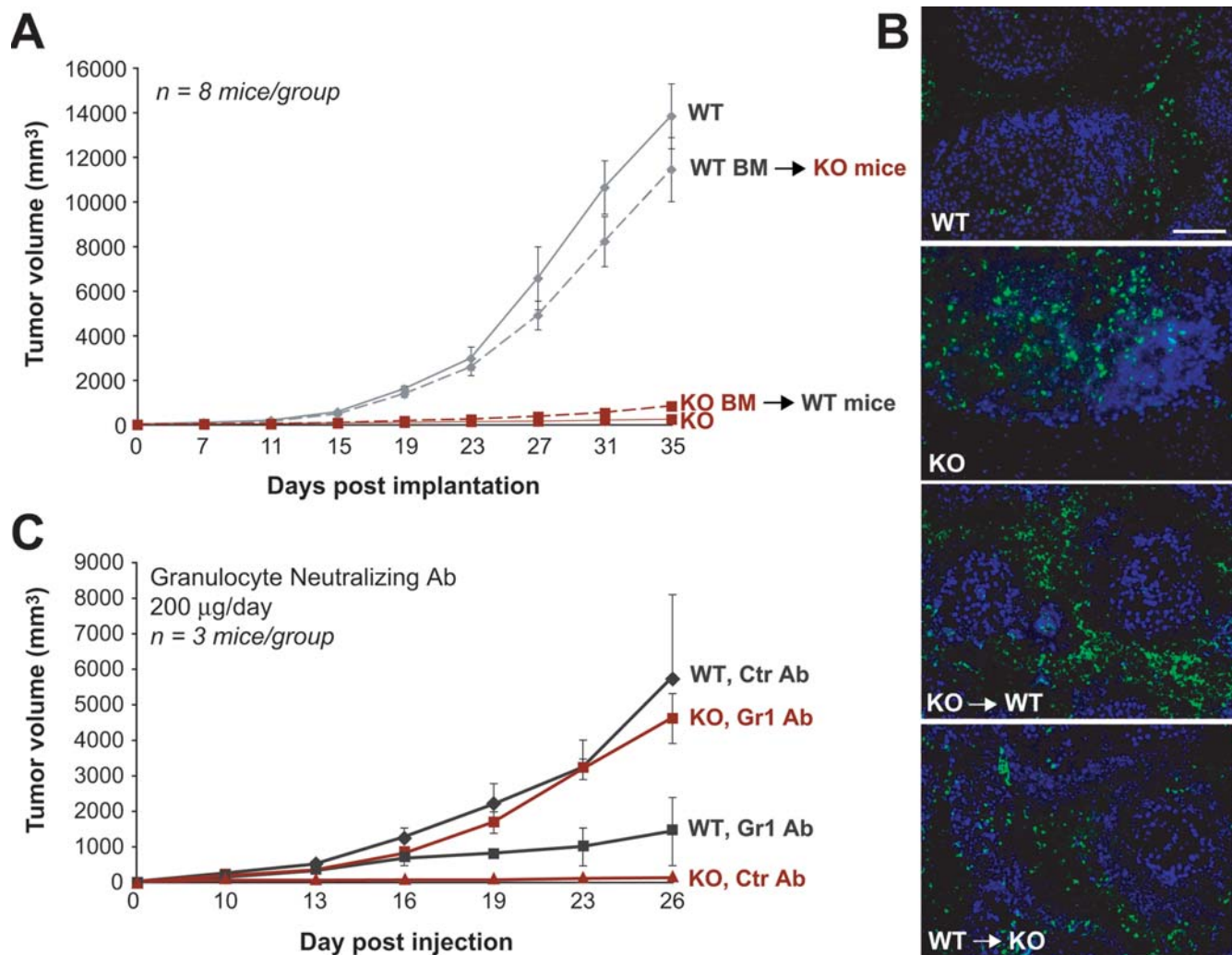


**Figure 4.** The inhibitory effect of PPAR $\alpha$  resides in the hematopoietic compartment. **(A)** B16-BL6 melanoma growth in WT mice receiving KO bone marrow (KO BM → WT mice) compared to PPAR $\alpha$  KO mice receiving WT bone marrow (WT BM → KO mice). WT bone marrow “rescues” tumor growth in PPAR $\alpha$  KO mice. **(B)** Subcutaneous B16-BL6 tumors on day 28 post-implantation show abundant CD45 staining in PPAR $\alpha$  WT mice receiving KO bone marrow (KO → WT). In B16-BL6 tumors in KO mice receiving WT bone marrow (WT → KO) CD45 staining (shown in green) was markedly reduced. Hoechst staining of nuclei is blue. Scale bar, 100 μm. **(C)** Effect of granulocyte depletion using Gr-1 antibody or control antibody (Ctr Ab, IgG2b) on B16-BL6 melanoma growth rate in PPAR $\alpha$  KO and WT mice.

doi:10.1371/journal.pone.0000260.g004

plantation experiments the PPAR $\alpha$  status of the transplanted bone marrow cells recapitulates the tumor phenotype of the host. However, it cannot be excluded that the suppressor activity carried by PPAR $\alpha$ -deficient bone marrow cells overrides a potential tumor stimulatory contribution of PPAR $\alpha$  in other, non-bone marrow derived host cells, such as from the local stroma.

### Depletion of Granulocytes in the PPAR $\alpha$ KO Mice Restores Tumor Growth

Immunohistological analysis of B16-BL6 tumors in WT mice transplanted with PPAR $\alpha$ -deficient bone marrow cells showed an intense increase in leukocyte staining, mimicking the intratumoral leukocyte profile of tumors grown in PPAR $\alpha$  KO mice (Figure 4B). This pronounced leukocyte infiltration in WT mice transplanted with PPAR $\alpha$ -deficient bone marrow cells suggests that the presence of PPAR $\alpha$  within the inflammatory cells prevents an overt inflammatory response to tumors. Histological and immunohistological analysis of the dormant tumors in PPAR $\alpha$  knockout

mice revealed that the leukocyte population was predominantly composed of granulocytes, mainly neutrophils (Figure S2B). To corroborate an active role of these PPAR $\alpha$ -deficient granulocytes in tumor suppression, we depleted them in the host animals. Flow cytometry analysis confirmed that the granulocyte-specific neutralizing antibody GR1 completely depleted neutrophils (Figure S2C). The anti-granulocyte antibody GR1 restored tumor growth rate in the PPAR $\alpha$  KO mice almost completely by day 26 (Figure 4C). In PPAR $\alpha$  KO mice that received the control antibody (IgG2b), tumor growth remained inhibited. Conversely, in WT mice the GR1 antibody suppressed tumor growth (Figure 4C vs. 4A), confirming the previous reports that neutrophils are necessary for tumor growth [2,3]. However, tumor inhibition was even stronger in WT animals whose bone marrow had been replaced with that of PPAR $\alpha$  KO mice (Figure 4A) as well as in PPAR $\alpha$  deficient hosts (Figure 4A and 4C), again suggesting that not only is PPAR $\alpha$  necessary for tumor growth, but that its absence confers a tumor suppressor activity on neutrophils.

## The Inhibitory Role of TSP-1 on Tumor Growth

We next asked why are tumor growth and angiogenesis inhibited by PPAR $\alpha$ -deficient leukocytes? Activated inflammatory cells promote angiogenesis, tumor cell proliferation and metastasis through the production of angiogenic mediators, growth factors, chemokines and proteases [2,24–26]. A connection between the positive and negative mediators of the inflammatory response, NF- $\kappa$ B and PPAR $\alpha$ , has recently been suggested, because PPAR $\alpha$  has been shown to repress NF- $\kappa$ B activity/expression [27]. However, this model disagrees with our result that PPAR $\alpha$ -mediated suppression of inflammation is permissive for tumor growth rather than inhibitory. Therefore, our finding suggests that PPAR $\alpha$  regulates an aspect of inflammation that is different from that controlled by NF- $\kappa$ B and hence, PPAR $\alpha$  modulation of inflammation affects tumor growth independently of NF- $\kappa$ B. While NF- $\kappa$ B exerts its tumor-promoting effect by induction of cytokines, we investigated whether PPAR $\alpha$  deficiency suppresses tumor growth by increasing the expression of the matrix protein thrombospondin-1 (TSP-1) which inhibits angiogenesis and stimulates granulocyte migration [28].

In fact, TSP-1 was elevated in the plasma and tumor tissue of PPAR $\alpha$  KO mice (Figure 5A and Figure S2D). Because TSP-1 can be expressed in several cell types, including tumor cells, endothelial cells and fibroblasts, we next determined the cellular origin for TSP-1 in the tumors of PPAR $\alpha$  deficient mice. B16-BL6 and B16-F10/GFP melanomas in PPAR $\alpha$  KO mice contained high levels of TSP-1 protein (Figure 5A), despite that these tumor cells do not express TSP-1 [29]. TSP-1 was found in tumors in PPAR $\alpha$  WT mice only when the mice received bone marrow from PPAR $\alpha$  KO animals. In contrast, little or no TSP-1 was detected in the tumors in PPAR $\alpha$  KO mice whose bone marrow cells had been replaced by those from PPAR $\alpha$  WT animals (Figure 5B). Moreover, in B16-BL6 tumors from PPAR $\alpha$  KO mice treated with GR1 antibody, little or no TSP-1 was detected (Figure 5C). Purified peripheral blood leukocytes from tumor-bearing PPAR $\alpha$  deficient mice expressed high levels of TSP-1 while WT leukocytes express very little if any TSP-1 (Figure 5D). Taken together, these findings suggest that in this model system, TSP-1 was produced predominantly by the inflammatory cells, and not by resident stromal cells.

To corroborate the role of TSP-1 in angiogenesis in PPAR $\alpha$  deficient animals, we performed the corneal neovascularization assay in the presence of neutralizing anti-TSP-1 antibody. Suppression of vessel length (endothelial cell migration and invasion) in PPAR $\alpha$  KO mice was partially reversed by inactivation of TSP-1 function (Figure 5E). There was no effect on the contiguous circumferential zone of the limbal vessel sprouting as measured by clock hours (Figure 5E). In contrast, in the WT mice, corneal neovascularization was not affected by the TSP-1 antibody (Figure 5E).

Provided that neovascularization is a valid marker for tumor angiogenesis, these results are in agreement with the established role of TSP-1 in tumor inhibition [30]. However, we found that the neutralizing TSP-1 antibody did not completely restore tumor growth in PPAR $\alpha$  KO mice to the level of that in WT mice,  $p < 0.02$  (Figure 5F). This may be either due to the limited access of TSP-1 antibody to the tumor bed or suggests that other endogenous inhibitors of angiogenesis may be involved. In fact, endostatin and IL-12 levels were significantly higher in PPAR $\alpha$  KO mice (data not shown). Unexpectedly, we found that in WT animals neutralization of TSP-1 also had an inhibitory (rather than promoting) effect on the tumor, suppressing tumor growth by approximately 71% when compared to control antibody-treated

mice,  $p < 0.02$  (Figure 5F). This suggests a complex, dualistic role of TSP-1 as a regulator of tumor growth.

## DISCUSSION

In this study we identified the cellular basis for the tumor suppressing phenotype of PPAR $\alpha$  deficient mice. Thus, PPAR $\alpha$  pathway represents a new link between inflammation, angiogenesis, and tumorigenesis. Absence of PPAR $\alpha$  in host granulocytes leads to inhibition of tumor growth, as demonstrated by: (1) transplantation of bone marrow cells from PPAR $\alpha$  KO mice to PPAR $\alpha$  WT mice and (2) by depletion of granulocytes by the neutralizing antibody, Gr1. Interestingly, PPAR $\alpha$  deficient granulocytes carried TSP-1, a protein that inhibits angiogenesis, leukocyte migration and tumor growth. When TSP-1 was depleted by neutralizing antibody in PPAR $\alpha$  KO mice, tumor growth was partially reversed.

PPAR $\alpha$  is best known as a critical regulator of lipid metabolism and inflammation [31], and is expressed in tissues that catabolize fatty acids such as the liver, as well as in various cell types including smooth muscle cells, monocyte/macrophages, lymphocytes, and endothelial cells [31]. PPAR $\alpha$  is the molecular target of the fibrate class of lipid-lowering drugs, which have been widely used for decades in the treatment of dyslipidaemia. Upon activation by PPAR $\alpha$  ligands, PPAR $\alpha$  heterodimerizes with retinoic acid receptor (RXR) regulating target gene expressions. PPAR $\alpha$  ligands act as PPAR $\alpha$  agonists. In addition to controlling lipid levels, they also function as potent anti-inflammatory agents in diseases such as atherosclerosis, colitis, and dermatitis [32–35]. Accordingly, PPAR $\alpha$  KO mice exhibit significant reduction of atherosclerotic lesions, delayed wound healing, and delayed liver regeneration [14,15,36], due to overt inflammatory processes. PPAR $\alpha$  deficiency also results in a prolonged inflammatory response to lipid mediators [8]. These findings collectively suggest that PPAR $\alpha$  has a physiological role in suppressing inflammation [7].

PPAR $\alpha$  agonists have been reported to induce liver tumors in rodents, but not in humans [10,37,38]. The mechanism for this species difference is still unclear. Accordingly, PPAR $\alpha$  KO mice are totally resistant to liver tumors induced by PPAR $\alpha$  ligands such as WY-14643 and clofibrate. This indicates that PPAR $\alpha$  is required for ligand-induced peroxisome proliferation and hepatocarcinogenesis in rodents in a cell-autonomous manner [9]. It is unclear to what extent this requirement of PPAR $\alpha$  for tumor growth is due to tumor cell-autonomous effects or its role in the host compartment of tumors, as shown by our current findings. In our experimental model the suppression of tumor growth in PPAR $\alpha$  KO mice is mediated by leukocytes, mainly neutrophils. PPAR $\alpha$  deletion is a second example for suppression of tumor growth by ablation of a gene in inflammatory cells; deletion of IKK $\beta$  in myeloid cells inhibits epithelial cell tumor growth [26]. However, our model does not exclude a contribution by cell-autonomous tumor promoting effects of PPAR $\alpha$ . In fact, we found that deletion of PPAR $\alpha$  in the tumor cell itself potentiated the tumor suppressing effect of PPAR $\alpha$ -deficiency in the host tissue (Figure 1G and H), in agreement with the earlier reports of the requirement for PPAR $\alpha$  in PPAR $\alpha$  agonist induced liver tumors [9]. Therefore, PPAR $\alpha$ , in addition to NF- $\kappa$ B, may represent another example of an oncogenic protein with a dual role in cancer by controlling essential functions both in cancer cell-autonomous processes as well as processes in the tumor bed, such as inflammation and angiogenesis. Oncogenes and NF- $\kappa$ B have been shown to stimulate tumor cell proliferation and angiogenesis by modifying cytokine expression profiles [25]. Therefore, PPAR $\alpha$  does not simply suppress inflammation, acting in opposition to NF- $\kappa$ B, but it does so in a qualitatively different manner in that

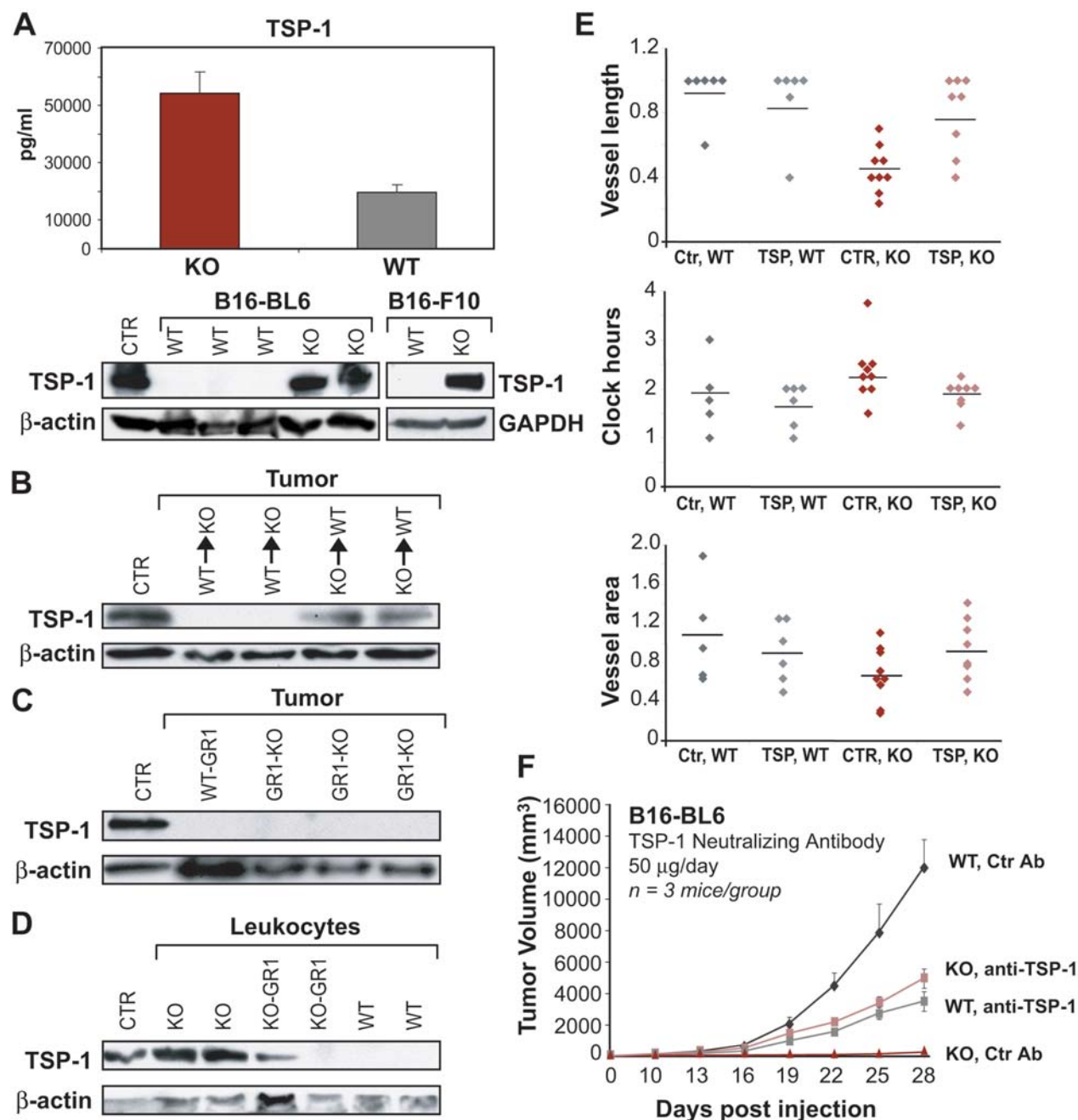


**Figure 5.** Effects of thrombospondin-1 (TSP-1) on angiogenesis and tumor growth in the PPAR $\alpha$ -deficient state. (A) First panel demonstrates TSP-1 levels in plasma of PPAR $\alpha$  KO and WT mice (ELISA); second panel shows TSP-1 levels in B16-BL6 and B16-F10/GFP tumor lysates at day 30 grown in PPAR $\alpha$  WT and KO mice (western blotting); positive CTR for TSP-1, proliferating HUVECs. (B) Western blot analysis of TSP-1 protein in B16-BL6 tumor lysates from PPAR $\alpha$  KO mice receiving WT bone marrow (WT BM $\rightarrow$ KO), and PPAR $\alpha$  WT mice receiving KO bone marrow (KO BM $\rightarrow$ WT); positive CTR for TSP-1, proliferating HUVECs. (C) TSP-1 protein expression is lost in B16-BL6 tumor lysates from PPAR $\alpha$  KO mice depleted of granulocytes (GR-1 antibody); positive CTR for TSP-1, proliferating HUVECs. (D) Western blot analysis of TSP-1 expression from isolated leukocytes from tumor-bearing PPAR $\alpha$  KO mice; positive CTR, proliferating HUVECs. Levels of  $\beta$ -actin demonstrate protein loading. (E) Effect of TSP-1 neutralizing antibody and control antibody (IgM) on vessel length (n=6–9 eyes), clock hours (n=5–9 eyes) and vessel area (n=5–9 eyes) in the corneal neovascularization assay. (F) B16-BL6 melanoma growth in KO and WT mice treated with TSP-1 neutralizing or control antibody (IgM). doi:10.1371/journal.pone.0000260.g005

cellular infiltrates that do not express PPAR $\alpha$ , actively suppress rather than stimulate tumor growth.

PPAR $\alpha$ -deficient leukocytes produce TSP-1, a potent inducer of leukocyte migration and inhibitor of angiogenesis. Thrombospondin-1 (TSP-1) is a trimeric glycoprotein (450kD) that has several functional domains with different binding affinities. It binds to

several cell surface receptors (CD36, integrins  $\alpha$ V $\beta$ 3,  $\alpha$ 3 $\beta$ 1,  $\alpha$ 4 $\beta$ 1,  $\alpha$ 5 $\beta$ 1, heparan sulfate proteoglycans) and also binds calcium and extracellular proteins, such as plasminogen, fibrinogen, fibronectin and urokinase [30,39]. This multitude of binding partners may explain the diversity of TSP-1 functions: TSP-1 modulates cell adhesion, migration, proliferation and differentiation regulating

processes such as inhibition of angiogenesis (through CD36 and  $\beta$ 1-integrin) and stimulation of neutrophil migration [28,40,41]. TSP-1 is expressed in several cell types in the host: platelets, neutrophils, monocytes, fibroblasts, pericytes, endothelial cells, and tumor cells [42]. Through its role as an activator of TGF- $\beta$ , it also modulates inflammatory reactions which may contribute to the lethality of TSP-1 KO mice [43]. TSP-1 inhibits tumor growth in mice when overexpressed, putatively via suppression of angiogenesis [40,44,45]. However, TSP-1 may also act as a promoter of tumor growth, because anti-TSP-1 receptor antibody inhibited breast tumor growth [46]. Moreover, *in vitro* TSP-1 has been shown to promote tumor cell invasion and chemotaxis [47–49]. In addition, further complicating the picture, in human plasma and tumor stroma the levels of TSP-1 have been correlated with both good and poor cancer prognosis [50–56]. This conflicting influence of TSP-1 is recapitulated in our animal model: TSP-1 delivered by leukocytes inhibited tumor growth. However, in the WT animals neutralization of TSP-1 also strongly inhibited tumor growth (Figure 5C). A possible explanation for this apparent paradox is that TSP-1 may have a biphasic effect on angiogenesis and leukocyte migration so that low doses (as found physiologically in WT animals) stimulate and high doses (present in PPAR $\alpha$  KO mice) inhibit these processes [57]. Such a “U-shape” dose-effect curve has been reported for many cytokines and bioactive molecules, such as interferon- $\alpha$ , PPAR $\gamma$  ligands and endostatin which all exhibit a biphasic effect on angiogenesis [58–62]. Therefore, in WT mice, TSP-1 may operate in the dose-effective window of promoting inflammation which in turn stimulates angiogenesis and tumor growth. In contrast, in PPAR $\alpha$  KO mice where TSP-1 is constitutively high, it would act as an inhibitor of tumor growth, perhaps through its antiangiogenic effects. Another possibility, technical rather than biological, is that the activity of TSP-1 is always inhibitory under the conditions studied, but the TSP-1 antibody itself generates the biphasic effect. High levels of TSP-1 in KO mice in the presence of TSP-1 antibodies may promote formation of large antigen-antibody complexes that facilitate TSP-1 clearance, while at low levels, as in WT mice, TSP-1 may be stabilized by the antibody [63].

Given the accumulating findings pointing to the importance for tumor growth of processes in non-cancer host tissues, such as angiogenesis, inflammation and other functions mediated by residual stroma and infiltrating bone marrow cells, our results add a new element to the emerging paradigm that tumor formation is not only a cell-autonomous process. Hence, the action of genes involved in tumor formation must be seen in the broader context of host and tumor [64]. While several pro-inflammatory factors stimulate tumor growth, we report a new molecular link between inflammation and cancer, in that abnormal inflammatory processes can inhibit tumor growth and angiogenesis - thus broadening the spectrum for anticancer therapies that aim at interfering with stromal processes.

## MATERIALS AND METHODS

### Tumor Xenograft Studies

All the animal studies were reviewed and approved by the animal care and use committee of Children's Hospital Boston. Three to six-month old male PPAR $\alpha$  knockout mice (129S4/SvJae), corresponding age-matched WT mice (129S1/SvIMJ, C57BL/6), obese WT mice (129S1/SvIMJ-retired breeders), C3H/HeJ and Balb/cJ mice were obtained from Jackson laboratories (Bar Harbor, ME). Retired WT breeders (35–40 gram) were used to control for weight as PPAR $\alpha$  KO mice become obese with age [65]. WT mice (129S4/SvJae) were provided by Dr. John

Heymach, Children's Hospital, Boston. PPAR $\alpha$  WT and KO littermates were F2 generation. For tumor studies, PPAR $\alpha$  negative (–/–) and PPAR $\alpha$  positive (+/+) tumors were developed by transforming mouse embryonic fibroblasts (embryonic day 11) isolated from PPAR $\alpha$  KO and WT mice, respectively, with SV40 large T-antigen and H-ras (generous gift from Dr. William Hahn). Tumor cells were injected subcutaneously ( $1 \times 10^6$  cells in 0.1 ml PBS). B16-BL6 melanoma cells were implanted directly from tissue culture; the growth of LLC and B16-F10/GFP tumors was achieved in 129 strains as follows: LLC and B16-F10/GFP cells were first grown in C57BL/6 mice and transplanted as pieces ( $1 \text{ mm}^3$ ) subcutaneously into PPAR $\alpha$  WT mice. When tumors were 1000–2000  $\text{mm}^3$ , they were serially passaged from mouse to mouse as  $1 \text{ mm}^3$  pieces and then grown in culture [59]. For experiments, LLC and B16-F10/GFP tumor cells were injected subcutaneously into the 129S PPAR $\alpha$  WT and PPAR $\alpha$  KO mice either from culture or from mouse to mouse as a cell suspension as described [59]. Tumors were measured every 3–5 days, and the volume was calculated as  $\text{width}^2 \times \text{length} \times 0.52$ . For metastasis studies, 500,000 cells in 0.1 ml PBS were injected via tail vein ( $n = 15$  mice/group). On day 21, when the PPAR $\alpha$  WT mice died, all remaining mice were euthanized. Histological sections of livers were quantified for liver metastasis ( $n = 34$ –53 fields). For corneal tumor studies, tumor pieces ( $1 \text{ mm}^3$ ) were implanted into the cornea, and the angiogenic response was recorded; photos were taken weekly using a slit-lamp microscope. For granulocyte depletion studies, GR-1 or control antibody (IgG2b) at 300  $\mu\text{g}/\text{mouse}$  (Biolegend, San Diego, CA) was administered intraperitoneally two days prior to B16-BL6 melanoma implantation in PPAR $\alpha$  WT and PPAR $\alpha$  KO mice, and every 3 days post-implantation. Granulocyte depletion was confirmed by flow cytometry using phycoerythrin conjugated Ly-6G (GR-1) antibody (Biolegend, San Diego, CA).

For neutralizing antibody experiments the A4.1 anti-TSP-1 monoclonal antibody (Lab Vision, Fremont, CA) (CSVTCG/CD36) or control antibody (IgM) at 50  $\mu\text{g}/\text{mouse}$  were administered intraperitoneally daily to PPAR $\alpha$  WT and KO mice in the corneal neovascularization and B16-BL6 melanoma experiments.

### Immunohistochemistry

Tumor samples were processed and immunohistochemical stainings were performed according to standard protocols [59]. For rat anti-mouse PECAM1 (BD Biosciences, San Jose, CA) staining, sections were treated with 40  $\mu\text{g}/\text{ml}$  proteinase K (Roche Diagnostics Corp.) for 25 minutes at 37°C. Detection of PECAM1 staining was completed using the tyramide amplification system according to the manufacturer's instructions (PerkinElmer, Boston, MA). For mouse monoclonal thrombospondin-1 (clone A6.1, Lab Vision, Fremont, CA) staining, sections were pretreated with pepsin for 15 minutes at 37°C (Biomed, Foster City, CA). For rat anti-mouse CD45 (BD Biosciences, San Jose, CA), and mouse monoclonal NP57 neutrophil elastase (Lab Vision, Fremont, CA) stainings no pretreatments were needed, and stainings were performed using Innogenex IHC kit (San Ramon, CA).

### Angiogenesis Assays

Corneal neovascularization assays were performed. Vessel length was the length of the vessels from the limbal vessel to the pellet. Vessel sprouting was measured as clock hours, the contiguous circumferential zone of the neovascularization, using a 360° reticule (where 30° of arc equals one clock hour). Vessel area was determined using the formula  $0.2\pi \times \text{vessel length} \times \text{clock hours of vessels}$  [66].



For *in vivo* Miles permeability assay, PPAR $\alpha$  WT and KO mice received an intravenous injection with 0.5% Evans blue dye (100  $\mu$ l) retro-orbitally. After ten minutes, the mice were given intradermal injections (50  $\mu$ l) into the dorsal skin or ear at 2 different sites, consisting of vehicle control or VEGF (50 ng; R&D Systems Inc., Minneapolis, MN). Twenty minutes later the dorsal skin and/or ears were harvested for densitometric analysis to quantify dye leakage. Columns represent mean  $\pm$  standard deviation ( $n = 6$  mice per group; experiments were performed three times).

### Transplantation of Bone Marrow Stem Cells

PPAR $\alpha$  WT and KO recipient mice were lethally irradiated with 14 Gy (in a split dose, 4 hours apart) 24 hours before bone marrow transplantation (BMT). Bone marrow cells ( $1 \times 10^6$ ) were injected retro-orbitally into recipient mice under isoflurane anesthesia. Neomycin sulfate antibiotic (2 mg/ml) was administered for two weeks post BMT in the drinking water. Mice recovered for a minimum of 2–3 months prior to tumor implantation.

### Western Blot Analysis

For preparation of tumor lysates from PPAR $\alpha$  WT and KO mice, B16BL6 tumors were homogenized with protease inhibitor (Roche, Germany). Total protein extracts (50  $\mu$ g) were analyzed on blots incubated with primary mouse monoclonal TSP-1 (Ab-11, Lab Vision, Fremont, CA) and HRP-conjugated secondary antibodies (Amersham Biosciences Corp. Piscataway, NJ). A positive control for TSP-1 was obtained from exponentially growing HUVECs. For isolation of leukocytes, peripheral blood of PPAR $\alpha$  WT and KO mice was obtained by retro-orbital bleeding under isoflurane anesthesia, red cells were cleared by incubating samples for 30 minutes on ice in red blood cell lysis buffer (Sigma-Aldrich, St. Louis, MO). Leukocytes were lysed in 100  $\mu$ l of a solution consisting of 20 mmol/L imidazole hydrochloride, 100 mmol/L KCl, 1 mmol/L MgCl<sub>2</sub>, 1 mmol/L EGTA, 1% Triton X-100, 10 mmol/L NaF, 1 mmol/L sodium molybdate, 1 mmol/L EDTA and protease inhibitor cocktail [67].

### TSP-1 ELISA

TSP-1 was measured by ELISA (Cytimmune, Rockville, MD) in blood plasma collected from non-tumor bearing PPAR $\alpha$  WT and KO mice. Blood was collected via retro-orbital puncture.

### Statistical Analyses

Statistical analyses were performed by Student's *t* test. The results were considered statistically significant for  $p < 0.05$ .

## SUPPORTING INFORMATION

**Figure S1** Tumor angiogenesis is inhibited in the cornea of PPAR $\alpha$  KO mice. PPAR $\alpha$  WT and KO host mice were implanted with tumor pieces (1 mm<sup>3</sup>) as indicated. (A) Comparison of PPAR $\alpha$ (+/+)MEF/RS and PPAR $\alpha$ (-/-)MEF/RS in WT mice day 9 and day 16. (B) PPAR $\alpha$ (+/+)MEF/RS and PPAR $\alpha$ (-/-)MEF/RS in PPAR $\alpha$  KO day 9 and day 16. The angiogenic

response of PPAR $\alpha$ (-/-)MEF/RS in PPAR $\alpha$  KO mice regressed by day 16. (C) Lewis Lung Carcinoma (LLC) in PPAR $\alpha$  WT and KO, C3H/HeJ and Balb/cJ on day 12. LLC tumors induced tumor angiogenesis independent of host haplotype. Therefore, major histo-incompatibility (MHC) does not prevent tumor-induced neovascularization and tumor growth. In contrast, LLC tumors failed to trigger any angiogenic response in PPAR $\alpha$  KO host. (D) B16-BL6 melanoma in PPAR $\alpha$  WT and KO on day 16. (E) Histology of B16-BL6 melanoma in the cornea of PPAR $\alpha$  WT and KO mice. Scale bars, 500  $\mu$ m (left) and 100  $\mu$ m (right) (F) Leukocyte (CD45, brown) staining of LLC tumors in the cornea of PPAR $\alpha$  WT and KO mice. Scale bar, 100  $\mu$ m.

Found at: doi:10.1371/journal.pone.0000260.s001 (8.59 MB TIF)

**Figure S2** (A) FACS analysis demonstrates % of CD45.1 host cells. In our bone marrow transplantation protocol, >90% of the hematopoietic system of the host was derived from the donor marrow (as proved by using CD45.1 mice as recipients and PPAR $\alpha$  KO mice that are CD45.2 as donors). (B) Panleukocyte (CD45, brown) and neutrophil elastase (red) staining in PPAR $\alpha$ (-/-)MEF/RS tumors in PPAR $\alpha$  WT (day 25) and PPAR $\alpha$  KO mice (day 55). Scale bar, 500  $\mu$ m. (C) FACS analysis demonstrates granulocyte depletion in PPAR $\alpha$  KO mice. (D) TSP-1 expression (brown) in B16-F10 (day 30) and PPAR $\alpha$ (-/-)MEF/RS (day 60) tumors in PPAR $\alpha$  KO and WT mice as determined by immunohistochemical staining. Scale bars, 100  $\mu$ m and 500  $\mu$ m, respectively.

Found at: doi:10.1371/journal.pone.0000260.s002 (5.12 MB TIF)

**Text S1** Genetic Background and Transplantation Immunity.

Found at: doi:10.1371/journal.pone.0000260.s003 (0.05 MB DOC)

## ACKNOWLEDGMENTS

We thank Deborah Freedman, Carmen Barnes, Michel Aguet, Thomas Boehm and Walter Wahli for helpful discussions in preparing the manuscript. We thank William Hahn for Large T- antigen and H-ras constructs. The excellent technical assistance of Andrea Laforme and Ricky Sanchez is acknowledged. We thank Kristin Johnson for photography.

## Author Contributions

Conceived and designed the experiments: SH DP AK. Performed the experiments: SH DP AK. Analyzed the data: SH DP AK. Contributed reagents/materials/analysis tools: SH. Wrote the paper: SH DP AK. Other: Participated in designing the studies and data analysis and participated in the intellectual input and discussions with AK and DP, and contributed to the writing of the paper: JF. Participated in designing the studies and data analysis and participated in the intellectual input and discussions with AK and DP and contributed to the writing of the paper: SH. Participated in designing all bone marrow transplantation and antibody depletion studies and performed the and contributed to the writing of the paper: GM. Participated in data analysis and the intellectual input and discussions with AK and DP: MK. Participated in designing the corneal assays and performed them: CB. Participated in designing all the metastasis assays and performed them: DB. Participated in designing the bone marrow transplantation experiments and the intellectual input and discussions with GM: RM.

## REFERENCES

- Bhowmick NA, Neilson EG, Moses HL (2004) Stromal fibroblasts in cancer initiation and progression. *Nature* 432: 332–337.
- Lin EY, Pollard JW (2004) Role of infiltrated leucocytes in tumour growth and spread. *Br J Cancer* 90: 2053–2058.
- de Visser KE, Eichten A, Coussens LM (2006) Paradoxical roles of the immune system during cancer development. *Nat Rev Cancer* 6: 24–37.
- Kammertoens T, Schuler T, Blankenstein T (2005) Immunotherapy: target the stroma to hit the tumor. *Trends Mol Med* 11: 225–231.

5. Zhang L, Conejo-Garcia JR, Katsaros D, Gimotty PA, Massobrio M, et al. (2003) Intratumoral T cells, recurrence, and survival in epithelial ovarian cancer. *N Engl J Med* 348: 203–213.
6. Pikarsky E, Porat RM, Stein I, Abramovitch R, Amit S, et al. (2004) NF-kappaB functions as a tumour promoter in inflammation-associated cancer. *Nature* 431: 461–466.
7. Staels B, Koenig W, Habib A, Merval R, Lebret M, et al. (1998) Activation of human aortic smooth-muscle cells is inhibited by PPARalpha but not by PPARgamma activators. *Nature* 393: 790–793.
8. Devchand PR, Keller H, Peters JM, Vazquez M, Gonzalez FJ, et al. (1996) The PPARalpha-leukotriene B4 pathway to inflammation control. *Nature* 384: 39–43.
9. Gonzalez FJ (2002) The peroxisome proliferator-activated receptor alpha (PPARalpha): role in hepatocarcinogenesis. *Mol Cell Endocrinol* 193: 71–79.
10. Peters JM, Cattley RC, Gonzalez FJ (1997) Role of PPAR alpha in the mechanism of action of the nongenotoxic carcinogen and peroxisome proliferator Wy-14,643. *Carcinogenesis* 18: 2029–2033.
11. Hays T, Rusyn I, Burns AM, Kennett MJ, Ward JM, et al. (2005) Role of peroxisome proliferator-activated receptor-alpha (PPARalpha) in bezafibrate-induced hepatocarcinogenesis and cholestasis. *Carcinogenesis* 26: 219–227.
12. Collett GP, Betts AM, Johnson MI, Pulimood AB, Cook S, et al. (2000) Peroxisome proliferator-activated receptor  $\alpha$  is an androgen-responsive gene in human prostate and is highly expressed in prostatic adenocarcinoma. *Clin Canc Res* 6: 3241–3248.
13. Thuillier P, Anchiraco GJ, Nickel KP, Maldve RE, Gimenez-Conti I, et al. (2000) Activators of peroxisome proliferator-activated- $\alpha$  partially inhibit mouse skin tumor promotion. *Mol Carcinog* 29: 134–142.
14. Michalik L, Desvergne B, Tan NS, Basu-Modak S, Escher P, et al. (2001) Impaired skin wound healing in peroxisome proliferator-activated receptor (PPAR)alpha and PPARbeta mutant mice. *J Cell Biol* 154: 799–814.
15. Tordjman K, Bernal-Mizrachi C, Zemany L, Weng S, Feng C, et al. (2001) PPARalpha deficiency reduces insulin resistance and atherosclerosis in apoE-null mice. *J Clin Invest* 107: 1025–1034.
16. Serrano M, Lin AW, McCurrah ME, Beach D, Lowe SW (1997) Oncogenic ras provokes premature cell senescence associated with accumulation of p53 and p16INK4a. *Cell* 88: 593–602.
17. Lyden D, Young AZ, Zagzag D, Yan W, Gerald W, et al. (1999) Id1 and Id3 are required for neurogenesis, angiogenesis and vascularization of tumour xenografts. *Nature* 401: 670–677.
18. Achilles EG, Fernandez A, Allred EN, Kisker O, Udagawa T, et al. (2001) Heterogeneity of angiogenic activity in a human liposarcoma: a proposed mechanism for "no take" of human tumors in mice. *J Natl Cancer Inst* 93: 1075–1081.
19. Udagawa T, Fernandez A, Achilles EG, Folkman J, D'Amato RJ (2002) Persistence of microscopic human cancers in mice: alterations in the angiogenic balance accompanies loss of tumor dormancy. *Faseb J* 16: 1361–1370.
20. Chang LK, Garcia-Cardena G, Farnbo F, Fannon M, Chen EJ, et al. (2004) Dose-dependent response of FGF-2 for lymphangiogenesis. *Proc Natl Acad Sci U S A* 101: 11658–11663.
21. Seghezzi G, Patel S, Ren CJ, Gualandris A, Pintucci G, et al. (1998) Fibroblast growth factor-2 (FGF-2) induces vascular endothelial growth factor (VEGF) expression in the endothelial cells of forming capillaries: an autocrine mechanism contributing to angiogenesis. *J Cell Biol* 141: 1659–1673.
22. Miles AA, Miles EM (1952) Vascular reactions to histamine, histamine-liberator and leukotaxine in the skin of guinea-pigs. *J Physiol* 118: 228–257.
23. Dvorak HF (2002) Vascular permeability factor/vascular endothelial growth factor: a critical cytokine in tumor angiogenesis and a potential target for diagnosis and therapy. *J Clin Oncol* 20: 4368–4380.
24. Coussens LM, Werb Z (2002) Inflammation and cancer. *Nature* 420: 860–867.
25. Sparmann A, Bar-Sagi D (2004) Ras-induced interleukin-8 expression plays a critical role in tumor growth and angiogenesis. *Cancer Cell* 6: 447–458.
26. Greten FR, Eckmann L, Greten TF, Park JM, Li ZW, et al. (2004) IKKbeta links inflammation and tumorigenesis in a mouse model of colitis-associated cancer. *Cell* 118: 285–296.
27. Delerive P, De Bosscher K, Besnard S, Vanden Berghe W, Peters JM, et al. (1999) Peroxisome proliferator-activated receptor alpha negatively regulates the vascular inflammatory gene response by negative cross-talk with transcription factors NF-kappaB and AP-1. *J Biol Chem* 274: 32048–32054.
28. Mansfield PJ, Boxer LA, Suchard SJ (1990) Thrombospondin stimulates motility of human neutrophils. *J Cell Biol* 111: 3077–3086.
29. Hamano Y, Sugimoto H, Soubasakos MA, Kieran M, Olsen BR, et al. (2004) Thrombospondin-1 associated with tumor microenvironment contributes to low-dose cyclophosphamide-mediated endothelial cell apoptosis and tumor growth suppression. *Cancer Res* 64: 1570–1574.
30. Lawler J, Detmar M (2004) Tumor progression: the effects of thrombospondin-1 and -2. *Int J Biochem Cell Biol* 36: 1038–1045.
31. Berger J, Moller DE (2002) Mechanism of action of PPARs. *Ann Rev Med* 53: 409–435.
32. Tanaka T, Kohno H, Yoshitani S, Takashima S, Okumura A, et al. (2001) Ligands for peroxisome proliferator-activated receptors  $\alpha$  and  $\gamma$  inhibit chemically induced colitis and formation of aberrant crypt foci in rats. *Cancer Res* 61: 2424–2428.
33. Neve BP, Fruchart JC, Staels B (2000) Role of the peroxisome proliferator-activated receptors (PPAR) in atherosclerosis. *Biochem Pharmacol* 60: 1245–1250.
34. Li AC, Brown KK, Silvestre MJ, Wilson TM, Palinski W, et al. (2000) Peroxisome proliferator-activated receptor  $\gamma$  ligands inhibit development of atherosclerosis in LDL receptor-deficient mice. *J Clin Invest* 106: 523–531.
35. Komuves LG, Hanley K, Lefebvre AM, Man MQ, Ng DC, et al. (2000) Stimulation of PPARalpha promotes epidermal keratinocyte differentiation in vivo. *J Invest Dermatol* 115: 353–360.
36. Anderson SP, Yoon L, Richard EB, Dunn CS, Cattley RC, et al. (2002) Delayed liver regeneration in peroxisome proliferator-activated receptor-alpha-null mice. *Hepatology* 36: 544–554.
37. Lee SS, Pineau T, Drago J, Lee EJ, Owens JW, et al. (1995) Targeted disruption of the alpha isoform of the peroxisome proliferator-activated receptor gene in mice results in abolishment of the pleiotropic effects of peroxisome proliferators. *Mol Cell Biol* 15: 3012–3022.
38. Cattley RC, DeLuca J, Elcombe C, Fenner-Crisp P, Lake BG, et al. (1998) Do peroxisome proliferating compounds pose a hepatocarcinogenic hazard to humans? *Regul Toxicol Pharmacol* 27: 47–60.
39. Bornstein P (2001) Thrombospondins as extracellular modulators of cell function. *J Clin Invest* 107: 929–934.
40. de Fraipont F, Nicholson AC, Feige JJ, Van Meir EG (2001) Thrombospondins and tumor angiogenesis. *Trends Mol Med* 7: 401–407.
41. Short SM, Derrien A, Narsimhan RP, Lawler J, Ingber DE, et al. (2005) Inhibition of endothelial cell migration by thrombospondin-1 type-1 repeats is mediated by beta1 integrins. *J Cell Biol* 168: 643–653.
42. Esemuede N, Lee T, Pierre-Paul D, Sumpio BE, Gahtan V (2004) The role of thrombospondin-1 in human disease. *J Surg Res* 122: 135–142.
43. Lawler J, Weinstein R, Hynes RO (1988) Cell attachment to thrombospondin: the role of ARG-GLY-ASP, calcium, and integrin receptors. *J Cell Biol* 107: 2351–2361.
44. Streit M, Velasco P, Brown LF, Skobe M, Richard L, et al. (1999) Overexpression of thrombospondin-1 decreases angiogenesis and inhibits the growth of human cutaneous squamous cell carcinomas. *Am J Pathol* 155: 441–452.
45. Weinstat-Saslow DL, Zabrenetzky VS, VanHoutte K, Frazier WA, Roberts DD, et al. (1994) Transfection of thrombospondin 1 complementary DNA into a human breast carcinoma cell line reduces primary tumor growth, metastatic potential, and angiogenesis. *Cancer Res* 54: 6504–6511.
46. Wang TN, Qian XH, Granick MS, Solomon MP, Rothman VL, et al. (1996) Inhibition of breast cancer progression by an antibody to a thrombospondin-1 receptor. *Surgery* 120: 449–454.
47. Crawford SE, Flores-Stadler EM, Huang L, Tan XD, Ranalli M, et al. (1998) Rapid growth of cutaneous metastases after surgical resection of thrombospondin-secreting small blue round cell tumor of childhood. *Hum Pathol* 29: 1039–1044.
48. Wang TN, Qian X, Granick MS, Solomon MP, Rothman VL, et al. (1996) Thrombospondin-1 (TSP-1) promotes the invasive properties of human breast cancer. *J Surg Res* 63: 39–43.
49. Albo D, Berger DH, Tuszynski GP (1998) The effect of thrombospondin-1 and TGF-beta 1 on pancreatic cancer cell invasion. *J Surg Res* 76: 86–90.
50. Tuszynski GP, Smith M, Rothman VL, Capuzzi DM, Joseph RR, et al. (1992) Thrombospondin levels in patients with malignancy. *Thromb Haemost* 67: 607–611.
51. Nathan FE, Hernandez E, Dunton CJ, Treat J, Switalska HI, et al. (1994) Plasma thrombospondin levels in patients with gynecologic malignancies. *Cancer* 73: 2853–2858.
52. Yamashita Y, Kurohiji T, Tuszynski GP, Sakai T, Shirakusa T (1998) Plasma thrombospondin levels in patients with colorectal carcinoma. *Cancer* 82: 632–638.
53. Grossfeld GD, Ginsberg DA, Stein JP, Bochner BH, Esrig D, et al. (1997) Thrombospondin-1 expression in bladder cancer: association with p53 alterations, tumor angiogenesis, and tumor progression. *J Natl Cancer Inst* 89: 219–227.
54. Ohta Y, Shridhar V, Kalemkerian GP, Bright RK, Watanabe Y, et al. (1999) Thrombospondin-1 expression and clinical implications in malignant pleural mesothelioma. *Cancer* 85: 2570–2576.
55. Mehta R, Kyshtobayeva A, Kurosaki T, Small EJ, Kim H, et al. (2001) Independent association of angiogenesis index with outcome in prostate cancer. *Clin Cancer Res* 7: 81–88.
56. Oshiba G, Kijima H, Himeno S, Kenmochi T, Kise Y, et al. (1999) Stromal thrombospondin-1 expression is correlated with progression of esophageal squamous cell carcinomas. *Anticancer Res* 19: 4375–4378.
57. Motegi K, Harada K, Pazouki S, Baillie R, Schor AM (2002) Evidence of a biphasic effect of thrombospondin-1 on angiogenesis. *Histochem J* 34: 411–421.
58. Slaton JW, Perrotte P, Inoue K, Dinney C, Fidler IJ (1999) Interferon- $\alpha$ -mediated down-regulation of angiogenesis-related genes and therapy of bladder cancer are dependent on optimization of biological dose and schedule. *Clin Cancer Res* 5: 2726–2734.
59. Panigrahy D, Singer S, Shen LQ, Butterfield CE, Freedman DA, et al. (2002) PPAR $\gamma$  ligands inhibit primary tumor growth and metastasis by inhibiting angiogenesis. *J Clin Invest* 110: 923–932.

60. Celik I, Surucu O, Dietz C, Heymach JV, Force J, et al. (2005) Therapeutic efficacy of endostatin exhibits a biphasic dose-response curve. *Cancer Res* 65: 11044–11050.
61. Hadley C (2003) What doesn't kill you makes you stronger. A new model for risk assessment may not only revolutionize the field of toxicology, but also have vast implications for risk assessment. *EMBO Rep* 4: 924–926.
62. Tjin Tham Sjin RM, Naspinski J, Birsner AE, Li C, Chan R, et al. (2006) Endostatin therapy reveals a U-shaped curve for antitumor activity. *Cancer Gene Ther.*.
63. Crommelin DJA, Sindelar RD (2002) Immunogenicity. In: Crommelin DJA, Sindelar RD, eds. *Pharmaceutical biotechnology : an introduction for pharmacists and pharmaceutical scientists*. 2nd ed. ed. New York: Routledge. pp. 125–127.
64. Dave SS, Wright G, Tan B, Rosenwald A, Gascoyne RD, et al. (2004) Prediction of survival in follicular lymphoma based on molecular features of tumor-infiltrating immune cells. *N Engl J Med* 351: 2159–2169.
65. Costet P, Legendre C, More J, Edgar A, Galtier P, et al. (1998) Peroxisome proliferator-activated receptor alpha-isoform deficiency leads to progressive dyslipidemia with sexually dimorphic obesity and steatosis. *J Biol Chem* 273: 29577–29585.
66. Kenyon BM, Voest EE, Chen CC, Flynn E, Folkman J, et al. (1996) A model of angiogenesis in the mouse cornea. *Invest Ophthalmol Vis Sci* 37: 1625–1632.
67. Joussen AM, Poulaki V, Qin W, Kirchhof B, Mitsiades N, et al. (2002) Retinal vascular endothelial growth factor induces intercellular adhesion molecule-1 and endothelial nitric oxide synthase expression and initiates early diabetic retinal leukocyte adhesion in vivo. *Am J Pathol* 160: 501–509.